Technological University Dublin

ARROW@TU Dublin

Articles

School of Mathematics

Stochastic particle acceleration in the lobes of giant radio galaxies

Stephen O'Sullivan
Technological University Dublin, stephen.osullivan@tudublin.ie

Brian Reville
Queen's University - Belfast

Andrew Taylor
Dublin Institute for Advanced Studies

Follow this and additional works at: https://arrow.tudublin.ie/scschmatart

Part of the Astrophysics and Astronomy Commons

Stochastic particle acceleration in the lobes of giant radio galaxies

S. O'Sullivan,[1][*] B. Reville[2] and A. M. Taylor[2]

[1]*School of Mathematical Sciences, Dublin City University, Dublin, Ireland*
[2]*Max-Planck-Institut für Kernphysik, 69029 Heidelberg, Germany*

ABSTRACT

We investigate the acceleration of particles by Alfvén waves via the second-order Fermi process in the lobes of giant radio galaxies. Such sites are candidates for the accelerators of ultra-high-energy cosmic rays (UHECR). We focus on the nearby Fanaroff–Riley type I radio galaxy Centaurus A. This is motivated by the coincidence of its position with the arrival direction of several of the highest energy Auger events. The conditions necessary for consistency with the acceleration time-scales predicted by quasi-linear theory are reviewed. Test particle calculations are performed in fields which guarantee electric fields with no component parallel to the *local* magnetic field. The results of quasi-linear theory are, to an order of magnitude, found to be accurate at low turbulence levels for non-relativistic Alfvén waves and at both low and high turbulence levels in the mildly relativistic case. We conclude that for pure stochastic acceleration via Alfvén waves to be plausible as the generator of UHECR in Cen A, the baryon number density would need to be several orders of magnitude below currently held upper limits.

Key words: acceleration of particles – plasmas – turbulence – cosmic rays – galaxies: active.

1 INTRODUCTION

The origin of ultra-high-energy ($\gtrsim 10^{18}$ eV) cosmic rays (UHECR) remains a long-standing mystery in high-energy astrophysics. A few objects are plausible as potential sources. In the Milky Way's $\sim\mu$G magnetic fields, for example, UHECR have gyroradii comparable to, or larger than, the size of the Galaxy. Moreover, the apparent isotropy in their arrival directions, at least up to $10^{19.7}$ eV, indicates that they must have propagated a sufficient distance to have undergone multiple scatterings. This clearly points to an extragalactic origin of UHECR.

Consideration of the possible sources for these particles has resulted in size, kinetic energy and magnetic field strength constraints (Hillas 1984), with it being possible to infer little more beyond this. Recent observations by the Pierre Auger Observatory (Auger) have indicated that UHECR with energies $>10^{19.7}$ eV appear to have statistically significant (at the 3σ level) correlations with the local (<75 Mpc) active galactic nuclei (AGN) distribution in the Veron–Cetty catalogue AGN population (Abraham et al. 2008). No such correlation was found in HiRes events (Abbasi et al. 2008), although the location of the observatory in the Northern hemisphere required analysis with a different AGN set from the catalogue. Nevertheless, such a signal is particularly interesting since it resides in the energy range where the propagation of UHECR becomes limited by GZK interactions (Greisen 1966; Zatsepin & Kuzmin 1967) to several hundreds of Mpc in distance, an effect which should make any such correlation easier to see.

One of the properties of cosmic rays at ultra-high energies is that, for $<$nG extragalactic fields, they are capable of propagating great distances (tens to hundreds of Mpc) in the intergalactic medium almost rectilinearly. One source of particular interest is Centaurus A, a Fanaroff–Riley type I (FR I) radio galaxy in the Southern hemisphere which has been associated with a number of Auger detections above $10^{19.7}$ eV: two with the centre itself (Abraham et al. 2008) and others with the extended lobes (Moskalenko et al. 2008). However, whether Cen A is merely deflecting particles towards our line of sight or is itself the site of acceleration is a topic of current interest (e.g. Gorbunov et al. 2008; Kotera & Lemoine 2008).

Within the AGN class of objects, several different acceleration sites present themselves as candidate locations for the acceleration of UHECR. Among these are the central AGN, the jet driving the lobe and the large radio lobes themselves (for a review, see Begelman, Blandford & Rees 1994). Furthermore, several acceleration mechanisms may be acting in parallel, with different processes dominating depending on the local conditions (Rieger, Bosch-Ramon & Duffy 2007). In particular, while first-order Fermi processes may be occurring near shocks, shear or inductive acceleration can operate in the jet (Ostrowski 1998; Rieger & Duffy 2004; Lyutikov & Ouyed 2007) and stochastic acceleration is likely to occur within the lobes.

In this paper, we consider the case of stochastic acceleration, it being responsible for the production of UHECR in giant radio galaxies. The lobes of these radio galaxies are most likely highly turbulent environments, where the fractional energy density in the magnetic turbulence, $\delta B^2/B_0^2$, is not necessarily a small parameter. Due to its size and estimated field strength, it has been argued

[*]E-mail: steve.osullivan@dcu.ie

by Hardcastle et al. (2008) that stochastic acceleration may be a possible mechanism for accelerating UHECR above 10^{19} eV in Cen A. It was assumed in this work that the magnetic energy density, $B_{tot}^2/8\pi$, was within 10 per cent of the rest mass energy density of the thermal protons in the lobe $0.5n_p m_p c^2$.

Earlier numerical studies of stochastic acceleration were mostly concerned with methods for solving the particle transport equation (e.g. Park & Petrosian 1996, and references therein) or the use of stochastic differential equations (Achterberg & Krülls 1992). Since tracking large ensembles of test particles is computationally expensive, previous investigations considered either the short time dependencies of diffusion characteristics on the turbulence level in a narrow dynamic range of $k_{max}/k_{min} = 10^3$ (Michałek & Ostrowski 1996; Michałek et al. 1999) or rapid acceleration in fully turbulent strong fields (e.g. Arzner et al. 2006). Attention has also been directed towards the influence of coherent acceleration processes invoked by means of an electric field component parallel to the local magnetic field (Dmitruk et al. 2003; Arzner et al. 2006). While parallel fields may be legitimately admitted via resistive processes in the magnetohydrodynamic(s) (MHD) fluid approximation, Arzner et al. (2006) have pointed out that if an electric field is generated via the Lorentz transformation of time-dependent Fourier modes representing magnetic fluctuations, an underestimate of the acceleration times may result as a consequence of finite local parallel electric fields.

An attempt at following the turbulent acceleration of protons in radio lobes over many decades in energy has recently been presented in Fraschetti & Melia (2008), although the acceleration time-scales resulting from their numerical scheme appear to disagree with quasilinear theory predictions by several orders of magnitude. Furthermore, their results, taken at face value, seem to be in conflict with the Hillas criterion, which limits the maximum particle energy E_{max} to which a given source can accelerate, $E_{max} = Ze\beta_A BcR$, where Z is the charge number, β_A is the Alfvén velocity in units of c, B is the magnetic field strength and R is the size of the source.

The goal of this paper is to use quasi-linear theory to place constraints on the parameters required to accelerate protons or ions to 10^{18} eV and above, assuming a homogeneous turbulent radio lobe. Numerical simulations are performed to check the accuracy of quasi-linear theory results when $\delta B^2/B_0^2$ and β_A are not small parameters. The outline of the paper is as follows. In Section 2, we review the basic results of stochastic acceleration using quasi-linear theory and discuss limitations on the acceleration time-scales for UHECR. Section 3 focuses directly on the acceleration of protons and electrons in the giant outer radio lobes of Cen A. In Section 4 we discuss the numerical model, demonstrating to what degree the results of quasi-linear theory hold in highly turbulent regions with non-linear magnetic turbulence or mildly relativistic Alfvén velocities. Our conclusions are presented in Section 5.

2 PARTICLE ACCELERATION IN TURBULENT FIELDS

The motion of a charged particle, with charge q, in electric and magnetic fields, E and B, respectively, is determined by the Lorentz force

$$\frac{d\boldsymbol{p}}{dt} = q(\boldsymbol{E} + \boldsymbol{\beta} \times \boldsymbol{B}), \qquad (1)$$

where $\boldsymbol{\beta}$ is the particle velocity normalized to the speed of light. Any change in the energy of a particle originates from the work

done by the E field. In most astrophysical environments, the local highly conducting plasma shorts out any large-scale electric field in the local fluid frame. However, for particles which cross back and forth across shocks there is no global frame in which all electric fields vanish. This is the underlying principle of diffusive-shock and shock-drift acceleration. In turbulent regions, it is the small-scale electric fields associated with the plasma waves that accelerate particles.

It was shown by Tverskoi (1967) that the evolution of the energetic particle distribution can be described by the momentum diffusion equation

$$\frac{\partial f(p,t)}{\partial t} = \frac{1}{p^2}\frac{\partial}{\partial p}\left[p^2 D(p)\frac{\partial f(p,t)}{\partial p}\right], \qquad (2)$$

which is valid for scattering time-scales much shorter than the crossing time of the physical system.

The form of the diffusion coefficient due to interactions with hydromagnetic waves has been discussed in detail in numerous publications (e.g. Kulsrud & Ferrari 1971; Schlickeiser 2002). We will focus on acceleration in a region of Alfvénic turbulence with a 1D power spectrum $W(k) \propto k^{-q}$, where $\delta B^2/8\pi = \int_{k_{min}}^{k_{max}} W(k)dk$, with $k = 2\pi/\lambda$. The wavenumbers k_{min} and k_{max} correspond to the longest (λ_{max}) and shortest (λ_{min}) wavelengths in the system, respectively. The spectral index of the power spectrum is denoted by q.

Neglecting numerical factors, and using the wave spectrum described above, the momentum diffusion coefficient is (Schlickeiser 1989)

$$D(p) \approx \beta_A^2 \frac{\delta B^2}{B_0^2}\left(\frac{r_g}{\lambda_{max}}\right)^{q-1}\frac{p^2c^2}{r_g c} \propto p^q, \qquad (3)$$

where $r_g = pc/eB_0$ is the gyroradius of a particle and β_A is the Alfvén velocity normalized to the speed of light. This result is valid for particles with gyroradii smaller than the correlation length of the field. The diffusion of particles with larger gyroradii is essentially independent of momentum since such particles interact with the entire spectrum (Tsytovich 1966). This results in an increase in acceleration times, a fact which we demonstrate numerically in Section 4. The associated mean free path, L, is

$$L \approx \frac{B_0^2}{\delta B^2}\left(\frac{r_g}{\lambda_{max}}\right)^{1-q} r_g. \qquad (4)$$

Equation (2) contains a systematic acceleration time-scale given by

$$t_{acc} = \frac{p^2}{D(p)} \approx \beta_A^{-2}\frac{L}{c} \propto p^{2-q}. \qquad (5)$$

For the rest of this section, we will consider exclusively a 1D Kolmogorov spectrum of Alfvén waves with $q = 5/3$ and a turbulence level $\delta B^2/B_0^2 = 1.0$. While Kolmogorov turbulent spectra are typical for such environments the actual value of the turbulence level is more difficult to determine, particularly in radio lobes where the magnetic Reynolds numbers are large. However, the results should be approximately accurate for gyroradii much less than the correlation length of the field since we calculate the Alfvén speed using the field's rms value.

For gyroradii larger than the correlation length of the turbulence, the acceleration rate falls off as p^{-2} (Berezinskii et al. 1990; Tsytovich 1966).[1] Hence, we consider the highest energy protons to

---

[1] Actually, the transition from $t_{acc} \propto p^{2-q}$ to $t_{acc} \propto p^2$ is smooth and starts to occur at gyroradii less than the correlation length $r_g < \lambda_c$, as shown in Section 4. Thus, the results that follow can be considered as rough upper limits.

be those which resonate with the largest wavelength in the system, $r_g/\lambda_{max} = 1$. The largest wave is taken to be an order of magnitude less than the size of the lobes $\lambda_{max} \approx 0.1\, R_{lobe}$. We note that the gyroradius for a proton of energy ε is $r_g \approx 10(\frac{\varepsilon}{10^{19}\mathrm{eV}})(\frac{B}{1\mu\mathrm{G}})^{-1}$kpc, such that for a radio lobe of size $R_{lobe} = 100$ kpc, and with $B = 1$ μG, protons of energy 10^{19} eV have gyroradii equal to λ_{max}. These parameters are in a range similar to those expected in the lobes of Cen A. We also note that protons with energy 10^{20} eV (in the same magnetic field) have gyroradii comparable to the size of the system, making the giant lobes of Cen A marginal candidates for the acceleration of UHECR to these energies, provided the particle has had sufficient time to reach these energies. According to equation (5), the corresponding acceleration time for such protons is $t_{acc}(\varepsilon_{max}) \sim \lambda_{max}/\beta_A^2 c$.

Using Faraday rotation measurements, upper limits can be estimated for the density in radio lobes. These are typically of the order $n_p = 10^{-4}$ cm^{-3} (Begelman et al. 1994), although the proton density can in fact be much lower. Adopting this upper value for the density in the lobe, the field and matter energy densities are roughly 0.025 eV cm^{-3} and 5×10^4 eV cm^{-3}, respectively, indicating an Alfvén speed of $\beta_A = (U_B/U_\rho)^{1/2} = 7 \times 10^{-4}$ where $U_B = B^2/8\pi$ and $U_\rho = 0.5 n_p m_p c^2$. Using these values, the acceleration time of a proton with energy $\varepsilon < \varepsilon_{max} = 10^{19}$ eV is

$$t_{acc} \approx 50 \left(\frac{\beta_A}{7 \times 10^{-4}}\right)^{-2} \left(\frac{\lambda_{max}}{10\mathrm{kpc}}\right)^{\frac{2}{3}} \left(\frac{\varepsilon}{10^{19}\,\mathrm{eV}}\right)^{\frac{1}{3}} \mathrm{Gyr}, \qquad (6)$$

which is longer than the Hubble time. Clearly, if ultra-high-energy protons are stochastically accelerated in radio lobes, the Alfvén speed must be considerably larger, that is lower density and/or higher magnetic fields. In fact, as we will demonstrate, for Cen A we require mildly relativistic Alfvén speeds $\beta_A \sim 0.1$.

We have so far neglected particle interactions with magnetosonic waves and acceleration due to transit-time damping (TTD). It is well known that fast-mode magnetosonic turbulence, when of comparable intensity to the Alfvén component, can present a more effective mechanism for particle acceleration through TTD (e.g. Schlickeiser & Miller 1998), the acceleration time being shorter by a factor ln (β_A^{-2}). However, this is still not sufficient to explain the acceleration of UHECR using the above canonical values for conditions in the lobes. Also, at Alfvén velocities $\beta_A \gtrsim 0.05$ the acceleration times become comparable.

Furthermore, as has been pointed out by Eichler (1979) and Achterberg (1981), acceleration by fast modes can become ineffective when $\beta > m_e/m_p$, where $\beta = P_{th}/U_B$ is the plasma beta parameter, with P_{th} being the sum of partial pressures. If the positron fraction of the plasma becomes significant, and the corresponding proton density drops, the electrons will dominate the total pressure. If β satisfies the above constraint, most of the wave energy goes into near-thermal particles and the fast modes are subject to rapid Landau damping. Assuming reasonable parameters for radio lobes, we find that $\beta \sim 1$ and therefore fast modes may be effectively dissipated. However, this remains a topic of on-going investigation (e.g. Yan & Lazarian 2004; Petrosian, Yan & Lazarian 2006).

It may be the case that TTD makes a significant contribution to particle acceleration in localized regions within the radio lobes. However, a large departure from canonical parameters is required in order to accelerate particles to the highest energies and, as discussed above, it is likely that scattering from Alfvénic turbulence is the dominant process for the highest energy particles. In the investigations presented here, we have therefore focused exclusively on Alfvén waves and defer to further studies the inclusion of fast-mode effects.

In Section 4, we investigate the accuracy of the acceleration time-scales for Alfvénic turbulence provided by quasi-linear theory for both non-relativistic and mildly relativistic Alfvén velocities, and for large $\delta B^2/B_0^2$. We emphasize here that the mildly relativistic models considered are highly speculative, involving ion densities three orders of magnitude below the upper limits derived from Faraday rotation measurements.

3 STOCHASTIC ACCELERATION IN CEN A

Cen A is the nearest radio galaxy and one of the brightest extragalactic radio sources in the sky (for a review see Israel 1998, and references therein). Concentrated within a circle of $20°$ around the nucleus of Cen A are 10 of the 27 reported events above $10^{19.7}$ eV. While two appear to come from the nucleus itself, many more coincide with its giant lobes (Moskalenko et al. 2008), which are approximately ~ 600 kpc in extent, and projected on the sky they have an angular size of $10°$. These correlations may well be deceptive with their sources possibly originating in the Centaurus supercluster (Gorbunov et al. 2008) or simply scattered into our line of sight by the magnetic fields in the galaxy or lobes (Kotera & Lemoine 2008).

Nevertheless, being the closest radio galaxy it has long been favoured as a source of UHECR (Farrar & Piran 2001; Isola, Lemoine & Sigl 2001). It was investigated in Hardcastle et al. (2008) whether these particles could be stochastically accelerated in the lifetime of the lobes. However, high Alfvén speeds were found to be necessary, in agreement with our discussion in Section 2. The actual value of the Alfvén velocity is uncertain. Using minimum energy arguments, the magnetic fields are not expected to exceed 3 μG in the giant lobes of Cen A (Alvarez et al. 2000).

Due to uncertainty in the baryon fraction of the particle content within the lobes, an accurate measurement of the density is a much more difficult task, with little more than upper limit estimates possible. While different upper limits have been given in different regions of the lobes based on the soft X-ray thermal emission, there is majority agreement at $\sim 10^{-4}$ cm^{-3} (for a review of different limits, see section 7.3 of Hardcastle et al. 2008). However, these are only upper limits and the actual densities may be considerably smaller.

Another uncertainty lies in the correlation length of the turbulence. While larger values allow for increased maximum proton energy, smaller values may favour rapid electron acceleration, provided the turbulent spectrum can extend to sufficiently short wavelengths to resonate with the electrons.

The turbulence is generated on large scales by hydrodynamic instabilities. Given the fact that the projected physical extent of each lobe is approximately 250 kpc $\times 100$ kpc, with a structure evident on all observed scales, a reasonable estimate of the correlation length is ~ 10 kpc.

The small-scale cut-off in the turbulent energy spectrum occurs at the scale l_{eq} at which equipartition between the kinetic and magnetic energies is reached. The correlation length may be in turn related to l_{eq} via the magnetic Reynolds number R_m according to $l_{eq} \approx R_m^{-1/2} l_{turb}$ (Ruzmaikin, Sokolov & Shukurov 1989). Assuming a characteristic bulk velocity of $0.1c$, and a temperature of 10^7 K, Spitzer (1962) provides an expression for transverse resistivity which yields a magnetic Reynolds number $R_m \sim 10^{35}$. Hence, $l_{eq} \ll r_{g\,thermal}$, where $r_{g\,thermal}$ is the gyroradius of thermal protons.

With $\lambda_{max} \approx 10$ kpc and $B \approx 3$ μG, a maximum energy of $\varepsilon_{max} \approx 10^{19.7}$ eV is indicated for $r_g \lesssim \lambda_{max}$, which is in the energy range relevant for the Auger events. The acceleration time for a particle of energy ε_{max} is $t_{acc} \approx 10^5\, \beta_A^{-2}$ yr, where we have assumed

a Kolmogorov spectrum $q = 5/3$ and equipartition between the energy density in the turbulent and ordered magnetic field.

The age of the radio lobes in Cen A is estimated to be $10^{7.5}$ yr (Hardcastle et al. 2008), which suggests that Alfvén speeds $\beta_A \gtrsim 0.1$ are necessary to accelerate particles to such high energies in the lifetime of the lobes. Again, assuming $B = 3\,\mu$G as an upper limit indicates that densities $\lesssim 10^{-7.5}\,$cm^{-3} are necessary to achieve such values of β_A.

3.1 Electron acceleration

As an interesting aside, one can calculate the acceleration time of electrons in the lobes of Cen A. We assume a turbulent spectrum with a uniform Kolmogorov power law extending to the length-scales required for resonance with radio emitting electrons. However, we note that the uncertainty associated with such an assumption is significant.

The combined radiative cooling time for electrons via synchrotron in a $3\,\mu$G magnetic field ($U_B = 0.2\,$eV cm^{-3}) and via inverse Compton in the cosmic microwave background (CMB) radiation field ($U_{CMB} \sim 0.3\,$eV cm^{-3}) is

$$t_{cool} = E_e / \frac{4}{3} c\sigma_T \beta_e^2 \gamma^2 U_{tot}$$

$$\approx 0.83 \left(\frac{\varepsilon}{10^{12}\,\text{eV}}\right)^{-1} \left(\frac{U_{tot}}{0.5\,\text{eV cm}^{-3}}\right)^{-1} \text{Myr}, \qquad (7)$$

where $U_{tot} = U_B + U_{CMB}$. The corresponding acceleration time for electrons is

$$t_{acc} \approx 25 \left(\frac{n_p}{10^{-4}\,\text{cm}^{-3}}\right) \left(\frac{\lambda_{max}}{10\,\text{kpc}}\right)^{\frac{2}{3}}$$

$$\times \left(\frac{U_B}{0.2\,\text{eV cm}^{-3}}\right)^{-\frac{7}{6}} \left(\frac{\varepsilon}{10^{12}\,\text{eV}}\right)^{\frac{1}{3}} \text{Myr}. \qquad (8)$$

Thus, cooling and acceleration time-scales for an electron become comparable at a critical energy

$$\varepsilon_c \approx 0.1 \left(\frac{n_p}{10^{-4}\,\text{cm}^{-3}}\right)^{-\frac{3}{4}} \left(\frac{\lambda_{max}}{10\,\text{kpc}}\right)^{-\frac{1}{2}}$$

$$\times \left(\frac{U_B}{0.2\,\text{eV cm}^{-3}}\right)^{\frac{7}{8}} \left(\frac{U_{tot}}{0.5\,\text{eV cm}^{-3}}\right)^{-\frac{3}{4}} \text{TeV}. \qquad (9)$$

Below this energy, the acceleration or re-acceleration of electrons may not be safely neglected.

Recently, Hardcastle et al. (2008) have presented results of the radio spectra from selected regions of Cen A in the northern and southern lobes. These authors fit models to the spectra in the southern regions using an inverse-Compton-cooled power-law spectrum, where the spectral age increases further from the nucleus (both spectral ages being $\sim 10^{7.5}$ yr). In the northern regions, the spectra obtained are different but can still be fitted with a continuous injection broken power-law model. The northern middle lobe is claimed to be responsible for the observed asymmetric behaviour. The spectral breaks are found, in all regions, to occur in the range 10^9–10^{10} Hz (corresponding to photon energies of 10^{-6}–10^{-5} eV). In the $\sim\mu$G fields that are assumed in the lobes, this corresponds to synchrotron radiating electrons with energies $\gtrsim 10^{10}$ eV, which falls below the critical value ε_c, although they could be consistent with a lower magnetic field value.

Interestingly, our value for ε_c was calculated using the upper limit for the number density. Lower densities such as those necessary for the stochastic acceleration of UHECR increase the value of ε_c by

several orders of magnitude, suggesting that stochastic acceleration may play an important role in the shape of the electron spectrum at these energies. More self-consistent calculations, similar to those of Kardashev (1962) and Stawarz & Petrosian (2008), are warranted to investigate this further.

Stochastic acceleration may also play an important role in the suggested re-acceleration of electrons observed near the hotspots of other radio galaxy jets (e.g. Meisenheimer 1996).

Finally, we reiterate that since the acceleration of 10^{10} eV electrons in a $3\,\mu$G field requires a Kolmogorov magnetic spectrum to span more than nine decades in length-scale with a uniform power law, any softening of the turbulence spectrum at large k will reduce the effects of stochastic acceleration. Hence, the large Alfvén speeds required to accelerate UHECR, as found in the previous section, are not necessarily in conflict with the radio spectra.

4 NUMERICAL TEST-PARTICLE SIMULATIONS

The quasi-linear results of Schlickeiser (1989) used in the previous section are calculated assuming purely resonant interactions with a continuous spectrum of non-relativistic Alfvén waves, $\beta_A \ll 1$, with total energy density $U_{turb} \ll U_B$. Since our results have taken these energy densities to be comparable, it is important to investigate the accuracy of the resulting expressions for the acceleration time.

Numerical investigations of stochastic acceleration in Alfvénic turbulence have previously been performed by Michałek & Ostrowski (1996) and Michałek et al. (1999). Their results show good agreement with quasi-linear theory although the simulations were limited in a dynamical range, focusing on a single energy in a narrow range of wavelengths. As yet, there has been no in-depth numerical study of the energy dependence of the acceleration times.

We calculate the acceleration time-scales of test particles in low-frequency Alfvénic turbulence, using an a priori field configuration which allows for time-dependent waves.

Two different approaches are adopted to determine these time-scales.

Direct simulation is carried out if acceleration is sufficiently rapid that the initial particle ensemble can be evolved from $\langle\gamma\rangle = 10^5$–$10^9$ within 4×10^7 gyroperiods (measured at the initial energy). This is the case for the mildly relativistic turbulence models we consider in this work.

If the acceleration time-scales are very long such that particle ensembles cannot be evolved over the range of interest in computationally viable simulations, we take *snapshots* of mono-energetic particle populations over the range and rely on the slow dispersion of the injected particle delta function distribution to derive early-time diffusion coefficients for Gaussian fits to the particle distribution. This is the case for the non-relativistic models.

We remark here that our investigations are limited to protons within the sample range $\langle\gamma\rangle = 10^5$–$10^9$. Since we wish to evaluate the plausibility of Alfvén-mediated stochastic acceleration as a mechanism for driving protons to ultra-high energies, viable acceleration time-scales over this range are a minimum necessary condition for acceleration from still lower energies.

We note that protons with energies less than 100 TeV will undergo stochastic acceleration provided they have sufficient energy to satisfy the resonance condition with short-wavelength Alfvén waves. This condition is necessary to facilitate the pitch angle scattering required for maintenance of a quasi-isotropic distribution.

We note that the accelerated particles require some pre-acceleration process to lift them from the thermal pool. However,

the consideration of pre-acceleration is beyond the scope of this paper.

4.1 Constructing the fields

We have extended the test-particle transport code LYRA (O'Sullivan et al. 2009) to include time-dependent magnetic fields and corresponding time-dependent electric fields.

A straightforward Lorentz transformation of magnetic fluctuations will, in general, lead to non-zero values of $\delta \boldsymbol{E} \cdot \boldsymbol{B}$. For the low-frequency waves we consider, this is unphysical and can lead to an unintended secular acceleration of the particle parallel to the local magnetic field (Arzner et al. 2006).

In this work, we shall consider two distinct field constructions which explicitly maintain $\delta \boldsymbol{E} \cdot \boldsymbol{B} = 0$. The first is a 1D field (in the sense that $\boldsymbol{k}$ is parallel or antiparallel to $\boldsymbol{B}_0$). In the second construction, $\boldsymbol{k}$ is isotropically orientated in 3D.

In each case, linear Alfvén turbulence is imposed upon a mean field, $\boldsymbol{B}_0$, by superimposing a large number of linearly polarized modes, $\delta \boldsymbol{B}_j (j = 1, \ldots, N)$, according to

$$\delta \boldsymbol{B}_j = A_j (\widehat{\boldsymbol{B}_0 \times \boldsymbol{k}_j}) \mathrm{e}^{\mathrm{i}(\boldsymbol{k}_j \cdot \boldsymbol{r} - \omega_j t + \phi_j)}, \tag{10}$$

where $\hat{\boldsymbol{k}}_j$ and ϕ_j are chosen randomly within the dimensionality constraints imposed upon the construction of the field as described below. The turbulent component of the field then approaches homogeneity and isotropy in the limit of large N (Batchelor 1982). The random selection of Fourier phases, ϕ_j, ensures that the field has no large-scale coherent structures, and the amplitudes A_j are chosen to create a Kolmogorov power spectrum. The waves are taken to be purely Alfvénic such that

$$\frac{\omega_j}{k_j c} = \beta_A |\cos \theta| \tag{11}$$

with θ being the angle between the wavevectors $\boldsymbol{k}_j$ and $\boldsymbol{B}_0$. Since the direction of $\boldsymbol{k}_j$ is determined using two angles in spherical polar coordinates, chosen at random, the absolute value of the cosine must be taken to prevent a directional bias in the fields.

4.1.1 One-dimensional field

In order to make contact with quasi-linear theory, we consider a simple 1D field construction similar to that used by Kulsrud & Pearce (1969), Schlickeiser (1989) and others, whereby weak perturbations have wavevectors purely parallel and antiparallel to the mean field. Explicitly, each wavevector is determined by a random sign selection

$$\hat{\boldsymbol{k}}_j^{\mathrm{1d}} = \pm \hat{\boldsymbol{B}}_0. \tag{12}$$

Vanishing $\delta \boldsymbol{E} \cdot \boldsymbol{B}$ is enforced by assuming a uniform linear polarization state for all modes. The polarization direction, $\widehat{\delta \boldsymbol{B}_1}$ say, is arbitrarily assigned perpendicularly to B_0 and then fixed for all remaining modes according to

$$\widehat{\delta \boldsymbol{B}_j} = \widehat{\delta \boldsymbol{B}_1} \quad \forall \quad j. \tag{13}$$

Via a Lorentz transformation, the associated electric field is

$$\delta \boldsymbol{E}_j = -\frac{\omega_j}{k_j} A_j (\hat{\boldsymbol{B}}_0 \times \widehat{\delta \boldsymbol{B}_j}) \mathrm{e}^{\mathrm{i}(\boldsymbol{k}_j \cdot \boldsymbol{r} - \omega_j t + \phi_j)}. \tag{14}$$

4.1.2 Three-dimensional field

Numerical investigations on the effects of anisotropy in the turbulent field have been reported by Michałek et al. (1999), by considering waves drawn randomly from within cones of differing opening angles about the mean field. They find that the diffusion coefficients vary by less than an order of magnitude.

However, it has also been argued by Goldreich & Sridhar (1995), Chandran (2000) and Cho & Lazarian (2002) that Alfvénic turbulence is anisotropic, with eddies elongated along the (local) mean magnetic field (i.e. $k_\perp > k_\parallel$). Yan & Lazarian (2004) have pointed out that this anisotropy can result in inefficient gyroresonant acceleration due to the reduction in the total power in parallel modes. The full importance of this effect is unclear in strongly turbulent fields, as may be prevalent in radio lobes.

For instance, there is observational evidence from polarization maps for chaotic fields in the southern lobe of Cen A (Junkes et al. 1993). Furthermore, lobes such as those of Cen A with morphologies characterized by extended filamentary structures (Carilli et al. 1989) are known to be weakly magnetized (Clarke 1996) in the sense that $\delta B > B_0$. Consequentially, hydrodynamic turbulence, as might arise from high velocity injection of plasma into the lobes, will result in a strongly chaotic magnetic field component.

We now describe the construction of a magnetic field from modes with wavevectors directed isotropically in 3D and a corresponding electric field such that $\delta \boldsymbol{E} \cdot \boldsymbol{B} = 0$.

Appealing to Ohm's law for an ideal plasma with infinite conductivity, we may write

$$\delta \boldsymbol{E} = -\delta \boldsymbol{u} \times \boldsymbol{B}, \tag{15}$$

where $\delta \boldsymbol{E}$, $\delta \boldsymbol{u}$ and $\boldsymbol{B}$ are the total electric, bulk plasma velocity in units of c and magnetic fields, respectively, in the observer frame.

Linearizing Faraday's law, and using the fact that linear Alfvén waves are non-compressional (ie. $\boldsymbol{k}_j \cdot \delta \boldsymbol{u}_j = 0$), we have

$$\delta \boldsymbol{u}_j = -\mathrm{sgn}(\cos \theta) \frac{\beta_A}{B_0} \delta \boldsymbol{B}_j \tag{16}$$

for the contribution to the velocity field due to each Alfvén mode. Hence,

$$\delta \boldsymbol{u} = -\frac{\beta_A}{B_0} (\boldsymbol{B}^+ - \boldsymbol{B}^-), \tag{17}$$

where $\boldsymbol{B}^+ (\boldsymbol{B}^-)$ is the sum of all forward (backward) moving modes with respect to the mean field. From equation (15),

$$\delta \boldsymbol{E} = -\delta \boldsymbol{u} \times \boldsymbol{B}_0 + 2 \frac{\beta_A}{B_0} (\boldsymbol{B}^+ \times \boldsymbol{B}^-). \tag{18}$$

Therefore, retaining the second-order correction to $\delta \boldsymbol{E}$ given by the second term on the right-hand side of equation (18) provides a total electric field satisfying $\delta \boldsymbol{E} \cdot \boldsymbol{B} = 0$. In the absence of this term, only $\delta \boldsymbol{E} \cdot \boldsymbol{B}_0 = 0$ and the electric field can still have a parallel component to the perturbing magnetic field, leading to rapid electrical acceleration of a charged particle propagating in the total B field, $\boldsymbol{B}$.

4.2 Equations of motion

Given the time-dependent fields $\boldsymbol{B}(\boldsymbol{r})$ and $\delta \boldsymbol{E}(\boldsymbol{r})$, the relativistic equations of motion for a particle of charge number Z, velocity $\boldsymbol{\beta} \equiv \boldsymbol{v}/c$ and rest mass m are

$$\frac{\mathrm{d}\gamma \boldsymbol{\beta}}{\mathrm{d}t} = \frac{Ze}{mc} (\delta \boldsymbol{E} + \boldsymbol{\beta} \times \boldsymbol{B}), \tag{19}$$

$$\frac{\mathrm{d}\boldsymbol{r}}{\mathrm{d}t} = \boldsymbol{\beta}c, \tag{20}$$

where e is the electronic charge. In a magnetic field of mean magnitude B_0, the characteristic relativistic Larmor angular frequency is $\omega_{\mathrm{g}} \equiv ZeB_0/\gamma mc$ where $\gamma \equiv (1 - \beta^2)^{-1/2}$. The corresponding maximal Larmor radius is $r_{\mathrm{g}} \equiv \omega_{\mathrm{g}}^{-1} \beta c$.

4.3 Simulations

To test the results presented in Section 2, we consider a homogeneous region of infinite extent with a mean field of $B_0 = 3\,\mu\mathrm{G}$ on to which an isotropic turbulent component δB is superimposed. The turbulence level of the field is determined via the parameter $(\sqrt{\langle \delta B^2 \rangle}/B_0)^2 \equiv (\delta B/B_0)^2$. The dynamic range of the turbulent field extends from $\lambda_{\min} = 10^{-8}$ kpc to $\lambda_{\max} = 1$ kpc and is resolved via 513 modes evenly spaced logarithmically. We have confirmed that our results are adequately converged at this mode density and dynamic range.

The Alfvén speed in the simulations is determined by the proton density according to

$$\beta_{\mathrm{A}} = \frac{1}{c} \frac{B_0}{\sqrt{4\pi m_{\mathrm{p}} n_{\mathrm{p}}}}, \tag{21}$$

where m_{p} and n_{p} are the proton mass and number density, respectively.

We consider eight different models in this work as defined by the parameters in Table 1. We consider non-relativistic turbulence $\beta_{\mathrm{A}} = 0.002$ for both low and high turbulence levels $(\delta B/B_0)^2 = 0.1$ and 1.0: models W and X, respectively. We also consider mildly relativistic turbulence $\beta_{\mathrm{A}} = 0.2$ for $(\delta B/B_0)^2 = 0.1$: model Y, and for $(\delta B/B_0)^2 = 1.0$: model Z. In each of these cases, both 1D and 3D Alfvén turbulence is considered.

For the non-relativistic models W and X, the acceleration time-scales are too long to capture the evolution of an injected particle distribution over a significant energy range with sufficient accuracy to resolve any statistical signal from numerical error. To see this, we have carried out benchmark integrations using a fifth-order adaptive Runge–Kutta method with the accuracy tolerance set to 10^{-6}.

For model X3, it takes approximately 1 h on an Intel Xeon 2.66 GHz CPU to achieve an integration over $6 \times 10^{-4}\,\tau_{\mathrm{acc}}(\gamma = 10^9)$ for a proton at $\gamma = 10^9$ or $4 \times 10^{-5}\,\tau_{\mathrm{acc}}(\gamma = 10^5)$ for a proton at $\gamma = 10^5$.

Therefore, for the non-relativistic models W and X, we rely on snapshots of the acceleration rate at energies $\log_{10} \gamma = \{5, 6, 7, 8, 9\}$. Furthermore, we find that integrations over $T = \{64, 32, 16, 8, 4\} \times 10^3 \omega_{0\,\mathrm{g}}^{-1}$, respectively, where $\omega_{0\,\mathrm{g}}(\gamma_0)$ is the relativistic Larmor frequency at the corresponding initial energy γ_0, are sufficient for the momentum distributions to complete the initial ballistic transport phase and become diffusive. While $t \ll \tau_{\mathrm{acc}}$, the

Table 1. Model parameters.

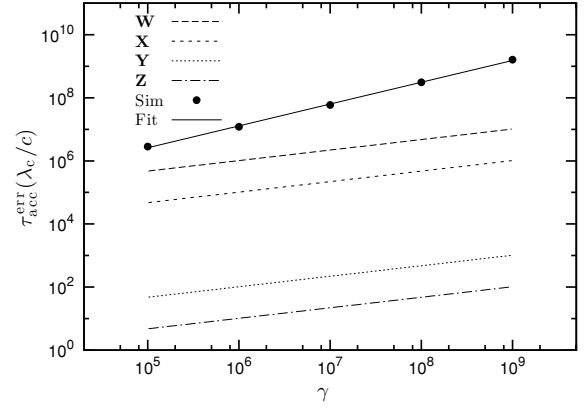| Model	Dimension	$(\delta B/B_0)^2$	n_{p} (cm^{-3})	β_{A}
W1	1	0.1	10^{-4}	0.002
W3	3	0.1	10^{-4}	0.002
X1	1	1.0	10^{-4}	0.002
X3	3	1.0	10^{-4}	0.002
Y1	1	0.1	10^{-8}	0.2
Y3	3	0.1	10^{-8}	0.2
Z1	1	1.0	10^{-8}	0.2
Z3	3	1.0	10^{-8}	0.2

Figure 1. Fictitious numerical acceleration $\tau_{\mathrm{acc}}^{\mathrm{err}}$ as a function of energy for 3D turbulence with the Runge–Kutta tolerance parameter $\epsilon = 10^{-6}$. τ_{acc} is derived from a systematic drift of momentum distribution via $\langle \Delta\gamma \rangle/\Delta t$. Simulation results for 765 particle ensembles at five different initial energies are indicated by filled circles. A best-fitting power law, $908\gamma^{0.69}$, is shown as a solid line. The expected values from quasi-linear theory for each of the case studies in this work are also represented via $C\gamma^{1/3}$: W – long dash – $C = 10224$; X – short dash – $C = 1022$; Y – dot – $C = 1.022$; Z – dot–dash – $C = 0.1022$.

momentum distributions may be approximated via Gaussian profiles. This can be easily demonstrated for the special case of a flat wave spectrum ($q = 1$) for which a solution to equation (2) is provided in Michałek & Ostrowski (1996). We consider termination times for integration ranging from $4 \times 10^{-4}\,\tau_{\mathrm{acc}}(\gamma = 10^5)$ for particles injected at $\gamma = 10^5$ to $1 \times 10^{-2}\,\tau_{\mathrm{acc}}(\gamma = 10^9)$ for particles injected at $\gamma = 10^9$.

It has been confirmed that energy is conserved to high accuracy by the integrator by examining its behaviour over characteristic integration times in the special case $\beta_{\mathrm{A}} = 0$ where $\tau_{\mathrm{acc}} \to \infty$. Under these conditions for 3D turbulence with $(\delta B/B_0) = 1.0$, energy is found to be conserved to within 0.005 per cent. Fig. 1 illustrates the systematic fictitious acceleration time-scales experienced by particles in this instance. Reference lines indicating quasi-linear theory predictions for the acceleration time-scales for each of the cases considered here are also shown. It is evident that, assuming the numerical errors do not grow disproportionately for $\beta_{\mathrm{A}} > 0$, sufficient numerical accuracy is employed to resolve the required signal from the statistical models.

For each of the W and X model snapshot energies, 1500 particles are injected with random position and velocity orientation in a randomly generated field. No more than three particles are released in any given realization in an effort to reduce numerical noise.

The mildly relativistic Y and Z models are less challenging numerically. This is because the acceleration time-scales are much shorter and therefore the integration can be carried out over a relatively long time. We inject 500 particles at $\gamma = 10^5$ for each of the 1D and 3D models and integrate continuously for $4 \times 10^7\,\omega_{0\,\mathrm{g}}(\gamma = 10^5)$. This is sufficient for acceleration to values of γ in excess of 10^9.

4.4 Non-relativistic turbulence

As previously remarked, for non-relativistic turbulence with $\beta_{\mathrm{A}} = 0.002$, integration over a large energy range is not feasible computationally. Instead, ensembles of particles are injected at discrete energies over the range of interest and instantaneous acceleration
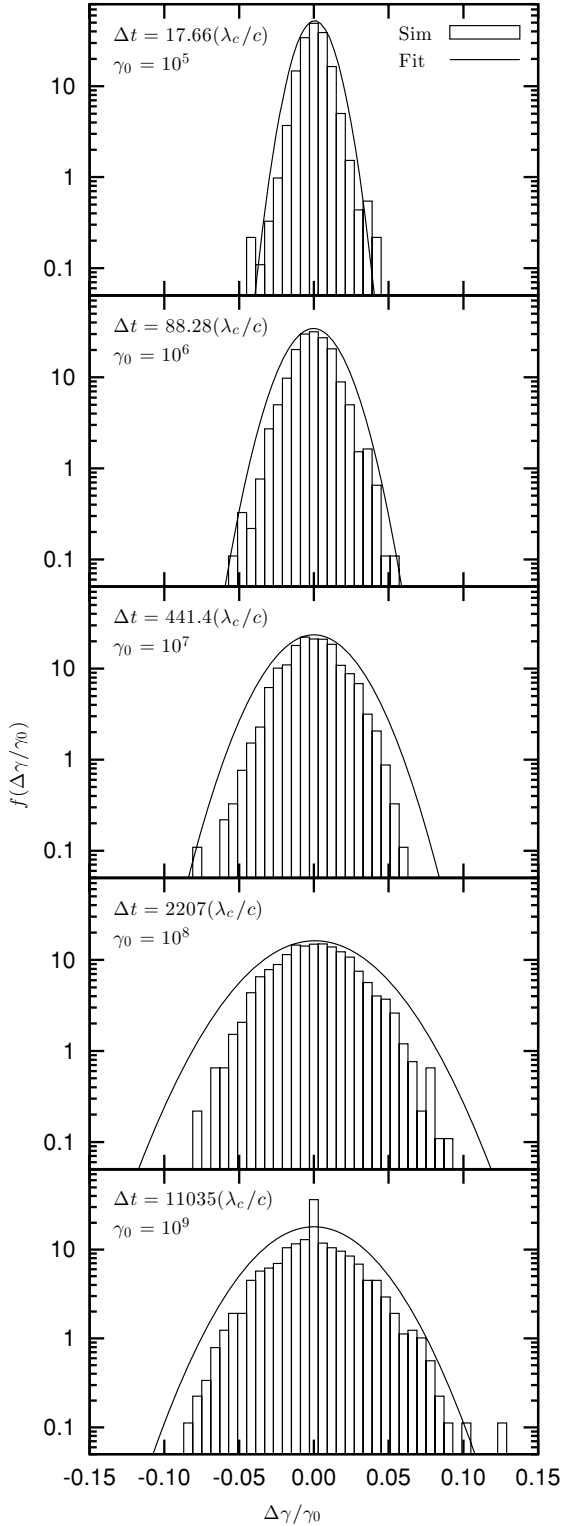
Figure 2. Model W1: histograms of relative energy change, $\Delta\gamma/\gamma_0$ (where $\Delta\gamma \equiv \gamma - \gamma_0$), for ensembles of 1500 mono-energetic protons injected at $t = 0$ with $\gamma = \gamma_0$. The solid line indicates a best-fitting Gaussian distribution: the mean drift $\langle\Delta\gamma\rangle$ and variance $\langle(\Delta\gamma)^2\rangle$ are given in Table 2.

times are inferred. This is achieved by allowing the injected delta function to relax to a Gaussian distribution and fitting its variance.

In Fig. 2, snapshots of the particle distributions are illustrated for the W1 model. The fitting parameters and errors are provided in

Table 2. Model W1: best-fitting Gaussian distribution parameters.

γ_0	$\sqrt{\langle(\gamma - \langle\gamma\rangle)^2\rangle}/\gamma_0$		$\langle\Delta\gamma\rangle/\gamma_0$	
10^5	0.0107	$\pm$ 0.0005	0.000506	$\pm$ 0.000583
10^6	0.0163	$\pm$ 0.0007	-0.000290	$\pm$ 0.000897
10^7	0.0239	$\pm$ 0.0011	0.000031	$\pm$ 0.001297
10^8	0.0343	$\pm$ 0.0015	0.000887	$\pm$ 0.001795
10^9	0.0314	$\pm$ 0.0025	0.000065	$\pm$ 0.003111

Table 2 for reference. Evidently, while the mean drift upwards in energy is overwhelmed by the error, the standard deviation is well captured to within ~ 5 per cent. We have confirmed that the variance of the distribution does indeed vary linearly after a few scattering times, τ_s, that is becomes diffusive. Furthermore, all simulated distributions achieve this diffusive phase of evolution with $\tau_s < l_c/c$ for $\rho < 1$ and $\tau_s \gtrsim l_c/c$ for the highest energy test cases.

The momentum diffusion coefficient is approximated by

$$D_p = \frac{\langle\Delta\gamma^2\rangle}{2\Delta t}, \tag{22}$$

where we have used the fact that the mean drift in the distribution is negligible over the integrated times, that is $\Delta\gamma = \gamma - \langle\gamma\rangle \approx \gamma - \gamma_0$. From this expression, the acceleration time, τ_{acc}, is then obtained using

$$\tau_{acc} = \frac{\gamma_0^2}{D_p}. \tag{23}$$

The results for the weakly turbulent models W1 and W3 are plotted in Figure 3. In both cases, an index of 0.36 is found for τ_{acc} using a best fit containing all points excluding that for the 10^9 ensemble. This is in close agreement with the theoretical value of 1/3 dictated by quasi-linear theory, although the index does appear to approach this value asymptotically for lower rigidities. Notably the 3D field presents acceleration times that are a factor of 4 larger than the 1D field case. This difference occurs due to the $\cos\theta$ dependence of the electric field strength for oblique Alfvén waves. The fact that the same normalization for the total turbulent power was used for both simulations, $\delta B^2/8\pi$, naturally accounts for the longer acceleration times. Comparing the results from the
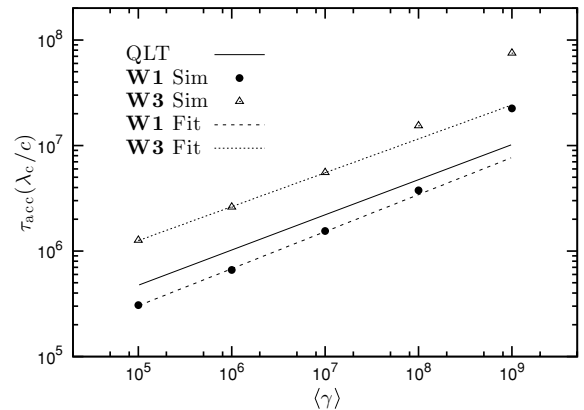

Figure 3. Models W: acceleration τ_{acc} as a function of energy. τ_{acc} is derived from best fits of Gaussian profiles to the standard deviation of the momentum distributions via γ_0^2/D_p where $D_p \equiv \langle\Delta\gamma^2\rangle/2\Delta t$. The expected value from quasi-linear theory, $10224\gamma^{1/3}$, is represented by the solid line. Note that for $\rho \equiv r_g/\lambda_c \gtrsim 1$, the efficacy of the acceleration process is damped. The best fit to the data for $\rho < 1$ ($\langle\gamma\rangle < 3.6 \times 10^8$) is given by $4531\gamma^{0.36}$ (dashed line) for W1 and $19138\gamma^{0.36}$ (dotted line) for W3.
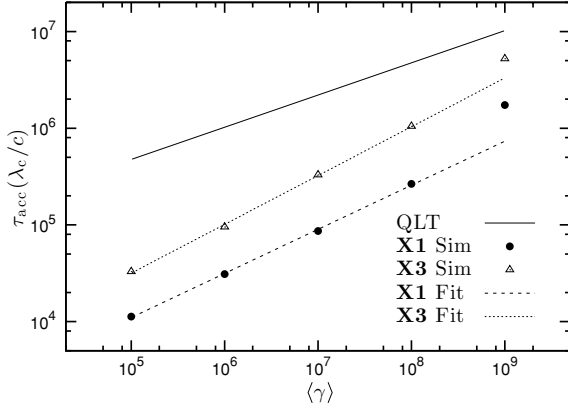
Figure 4. Models X: acceleration $\tau_{\rm acc}$ as a function of energy. $\tau_{\rm acc}$ is derived from best fits of Gaussian profiles to the standard deviation of the momentum distributions via γ_0^2/D_p, where $D_p \equiv \langle \Delta \gamma^2 \rangle / 2\Delta t$. The expected value from quasi-linear theory, $1022\gamma^{1/3}$, is represented by the solid line. Note that for $\rho \equiv r_{\rm g}/\lambda_{\rm c} \gtrsim 1$, the efficacy of the acceleration process is damped. The best fit to the data for $\rho < 1$ ($\langle \gamma \rangle < 3.6 \times 10^8$) is given by $58\gamma^{0.46}$ (dashed line) for X1 and $95\gamma^{0.50}$ (dotted line) for X3.

1D simulations with the quasi-linear theory result, we note that the numerically determined acceleration time is faster by a factor of almost 2. This may be due to the fact that the particles in our simulations can resonate with higher harmonics not accounted for in quasi-linear theory or simply that the turbulence level is not low enough. Nevertheless, the results in all cases are in good agreement to an order of magnitude.

It is also observed that for $\rho \gtrsim 1$ ($\gamma \gtrsim 3.6 \times 10^8$), the acceleration time strongly diverges from the theoretical result as particles' gyromotions exceed the scale at which resonant waves are present in the field.

Regarding the acceleration of UHECR, this emphasizes the fact that the maximum energy is quite typically governed by the correlation length of the field.

For models X1 and X3, where the turbulence level is high, the agreement with quasi-linear theory is less compelling, as illustrated in Figure 4. Here, the indices found are 0.46 and 0.50 for the 1D and 3D cases, respectively, and the experimentally determined acceleration times in both cases are also an order of magnitude faster than predicted in quasi-linear theory. The divergence from quasi-linear theory values with an increasing turbulence level is not surprising, as formally quasi-linear theory is valid in the limit of weak perturbations to the mean field. Again, the 3D field shows acceleration times longer than the 1D case by a factor of $\sim$4.

4.5 Mildly relativistic turbulence

For the mildly relativistic models Y and Z, with $\beta_{\rm A} = 0.2$, $n_{\rm p}$ has been set to $10^{-8}\,{\rm cm}^{-3}$, a value four orders of magnitude below Faraday rotation upper limits. While this value may be extreme, we wish to demonstrate the conditions under which second-order Fermi acceleration via pure Alfvénic turbulence is viable in our idealized model. We note that such low densities require a large fraction of positrons in order to safely neglect the influence of fast modes, as discussed in Section 2.

We find that for models Y and Z, the systematic acceleration is strong enough that we may simulate the acceleration of a single ensemble of particles from a low injection energy, $\gamma_0 = 10^5$, up to values of $\lesssim 10^{10}$. Furthermore, fewer particles are required in
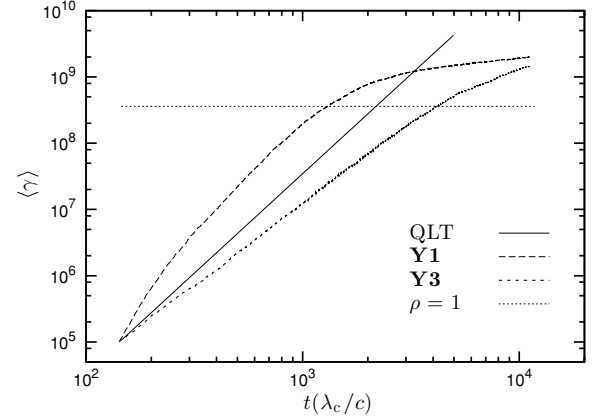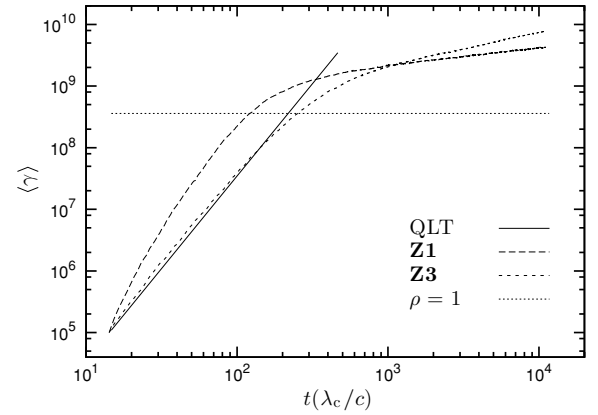

Figure 5. Models Y: mean energy against time for ensembles of 510 particles injected at $\gamma_0 = 10^5$. Reference line indicates $\rho = 1$. Quasi-linear theory result is $\langle \gamma \rangle = 0.03465t^3$. Y1 numerical results are indicated by long-dashed line and Y3 numerical results are indicated by short-dashed line. The critical energy 3.6×10^8 at which $\rho = 1$ is indicated by a dotted line.

Figure 6. Models Z: mean energy against time for ensembles of 500 particles injected at $\gamma_0 = 10^5$. The reference line indicates $\rho = 1$. Quasi-linear theory result is $\langle \gamma \rangle = 34.65t^3$. Z1 numerical results are indicated by long-dashed line and Z3 numerical results are indicated by a short-dashed line. The critical energy 3.6×10^8 at which $\rho = 1$ is indicated by a dotted line.

order to derive a smooth signal. In practice, this corresponds to integrations of 500 particles per model over $4 \times 10^7 \, \omega_{\rm g}^{-1} \, (\gamma_0)$.

The result from the mild relativistic turbulence models are plotted in Fig. 5 and Fig. 6. In both cases, the 1D field models, Y1 and Z1, exhibit more rapid acceleration than predicted by quasi-linear theory, with the low and high turbulence cases showing similarly curved profiles above the predicted $\langle \gamma \rangle \sim t^3$ power law. However, due to the relatively rapid acceleration in the plane perpendicular to the mean field, isotropy of the particle distribution cannot be maintained. As such, comparisons with the results of quasi-linear theory are misleading.

The mean energy plots for the 3D field models, Y3 and Z3, have flatter profiles. The high turbulence model is in excellent agreement with quasi-linear theory and the lower turbulence level case has a somewhat slower growth rate than predicted by theory.

As before, in all cases, once $\rho \gtrsim 1$, the acceleration is severely damped by lack of resonant scales in the field.

5 CONCLUSIONS

The stochastic acceleration of UHECR due to Alfvénic turbulence in the lobes of giant radio galaxies has been considered. The work is motivated by the recently reported correlation between a number of the highest energy events observed by the Pierre Auger observatory and nearby AGN. Making simple estimates, based on the results of quasi-linear theory, we have investigated the maximum energies that can be achieved with the use of reasonable parameters in radio lobes.

While the maximum possible energy that can be achieved in each lobe is primarily determined by the coherence length of the magnetic field in the lobes, the time-scale to achieve this is largely determined by the Alfvén speed. Assuming homogeneity of all quantities throughout the entire lobe, we have placed constraints on the value of the Alfvén speed necessary to stochastically accelerate particles 10^{18} eV within the lifetime of the lobes.

We have demonstrated that Alfvén speeds in excess of $0.1c$ are required in Centaurus A to accelerate cosmic rays above 10^{19} eV, although heavier nuclei could, in principle, achieve even higher energies. Also, should the composition of UHECRs with energies above 10^{19} eV be dominated by heavier nuclei, the observed UHE-CRs could be accelerated in the lobes of Cen A with an Alfvén speed which is an order of magnitude smaller. While the absolute value of the magnetic field strength in the lobes is quite well constrained by minimum energy arguments to fall in the range ~ 0.1–3 µG, the densities referred to in the literature are merely upper limits and indeed the proton number density could be considerably lower.

Provided the turbulence spectrum steepens considerably at smaller wavelengths, such high Alfvén velocities are not in conflict with the synchrotron radio emission from the non-thermal electrons. Conversely, should the Kolmogorov spectrum extend to sufficiently small wavelengths, the resulting rapid acceleration time of electrons might present a problem to the standard picture of an injected power law with a cooling break.

We have not allowed for TTD in the studies presented here since fast magnetosonic waves are not included in the turbulent field. While this simplifies the model and its interpretation, it may be justified by considering the efficacy of energy losses from these modes through heating of near-thermal electrons via Landau resonance effects. A comprehensive study of the linear theory of stochastic acceleration using a fully relativistic approach is, to our knowledge, still lacking, but a naive extension of the non-relativistic results to mildly relativistic phase velocities suggest that acceleration by Alfvén waves dominates above $\beta_A \sim 0.1$.

The numerical results presented in this work demonstrate purely stochastic acceleration of relativistic charged particles through interaction with linearly polarized Alfvén waves. The ideal MHD constraint, $\delta \boldsymbol{E} \cdot \boldsymbol{B} = 0$, is trivially maintained for fields with perturbations directed parallel to the mean field (1D) and by deriving an appropriate electric field from inferred velocity perturbations via Ohm's law for an ideal plasma (3D). For both these 1D and 3D field configurations we consider low and high turbulence levels, $(\delta B / B_0)^2 = 0.1, 1.0$, for non-relativistic and mildly relativistic turbulence, $\beta_A = 0.002, 0.2$, respectively.

For non-relativistic turbulence, we find that agreement with quasi-linear theory is good at low turbulence levels. The 3D acceleration time-scales are found to be in excess of quasi-linear theory by a factor of ~ 2. At higher turbulence levels, this agreement is less pronounced with the power-law dependence of the acceleration time on the energy becoming steeper. Over the range considered in this work, the absolute acceleration times are also shorter than predicted

by quasi-linear theory with approximately the same relative difference between the 1D and 3D cases.

Notably, above the critical energy corresponding to resonance with the largest wave in the system, $\rho = 1$, the particles interact with the entire Alfvén spectrum such that the diffusion becomes almost independent of energy. This dramatically reduces the efficacy of the acceleration process.

For the simulations with mildly relativistic Alfvén speeds, the mean energy of the particle ensembles shows reasonable agreement with quasi-linear theory up to $\rho = 1$ for both low and high turbulence levels. The 1D cases have more rapid acceleration than predicted by theory, but the distributions become anisotropic, and comparisons with quasi-linear theory are not applicable.

Given that the results of the numerical simulations are in reasonable agreement with the results of quasi-linear theory, in the mildly relativistic regime, the conditions necessary for stochastic acceleration of UHECR in Cen A can be satisfied, provided that the correlation length of the magnetic field is sufficiently large and that a particle can remain inside the lobe for a sufficiently long length of time. Paramount to this result is the relative low density of baryons in the lobes, which must fall considerably below the upper limits inferred from observations.

REFERENCES

Abbasi R. U., et al. (HiRes collaboration), 2008, preprint (arXiv:0804.0382)
Abraham J., et al. (Pierre Auger Collaboration), 2008, Astropart. Phys., 29, 188
Achterberg A., 1981, A&A, 97, 259
Achterberg A., Krülls W. M., 1992, A&A, 265, L13
Alvarez H., Aparici J., May J., Reich P., 2000, A&A, 355, 863
Arzner K., Knaepen B., Carati D., Denewet N., Vlahos L., 2006, ApJ, 637, 322
Batchelor G. K., 1982, The Theory of Homogeneous Turbulence, Cambridge Univ. Press, Cambridge
Begelman M. C., Blandford R. D., Rees M. J., 1994, Rev. Mod. Phys., 56, 255
Berezinskii V. S., Bulanov S. V., Dogiel V. A., Ginzburg V. L., Ptuskin V. S., 1990, Astrophysics of Cosmic Rays. North-Holland Publishing, Amsterdam
Carilli C. L., Dreher J. W., Conner S., Perley R. A., 1989, AJ, 98, 513
Chandran B. D. G., 2000, Phys. Rev. Lett., 85, 4656
Cho J., Lazarian A., 2002, Phys. Rev. Lett., 88, 5001
Clarke D. A., 1996, in Hardee P. E., Bridle A. H., Zensus J. A., eds, ASP Conf. Ser. Vol. 100, Energy Transport in Radio Galaxies and Quasars, Astron. Soc. Pac., San Francisco, p. 311
Dmitruk P., Matthaeus W. H., Seenu N., Brown M. R., 2003, ApJ, 597, L81
Eichler D., 1979, ApJ, 229, 409
Farrar G., Piran T., 2001, in Wheeler J. C., Martel H., eds, AIP Conf. Proc. Vol. 586, Relativistic Astrophysics: 20th Texas Symposium. Am. Inst. Phys., New York, p. 850
Fraschetti F., Melia F., 2008, MNRAS, 391, 1100

Goldreich P., Sridhar S., 1995, ApJ, 438, 763

Gorbunov D. S., Tinyakov P. G., Tkachev I. I., Troitsky S. V., 2008, JE TP Lett., 87, 461

Greisen K., 1966, Phys. Rev. Lett., 16, 748

Hardcastle M. J., Cheung C. C., Feain I. J., Stawarz L., 2008, MNRAS, 393, 1041

Hillas M., 1984, A&A, 22, 425

Isola C., Lemoine M., Sigl G., 2001, Phys. Rev. D., 65, 023004

Israel F. P., 1998, A&AR, 8, 237

Junkes N., Haynes R. F., Harnett J. I., Jauncey D. L., 1993, A&A, 269, 29

Kardashev N. S., 1962, SvA, 6, 317

Kulsrud R., Pearce W. P., 1969, ApJ, 156, 445

Kulsrud R. M., Ferrari A., 1971, Ap&SS, 12, 302

Kotera K., Lemoine M., 2008, Phys. Rev. D., 77, 3003

Lyutikov M., Ouyed R., 2007, Astropart. Phys., 27, 473

Meisenheimer K., 1996, in Kundt W., ed., Jets from Stars and Active Galactic Nuclei (Lecture Notes in Physics 471). Springer, Berlin, p. 57

Michałek G., Ostrowski M., 1996, Nonlinear Proc. Geophys., 3, 66

Michałek G., Ostrowski M., Schlickeiser R., 1999, Solar Phys., 184, 339

Moskalenko I. V., Stawarz Ł., Porter T. A., Cheung C. C., 2009, ApJ, 693, 1261

Ostrowski M., 1998, A&A, 335, 134

O'Sullivan S., Duffy P., Blundell K. M., Binney J., 2009, Phys. Rev. D, submitted

Park B. T., Petrosian V., 1996, ApJS., 103, 255

Petrosian V., Yan H., Lazarian A., 2006, ApJ, 644

Rieger F., Duffy P., 2004, ApJ, 617, 155

Rieger F., Bosch-Ramon V., Duffy P., 2007, Ap&SS, 309, 119

Ruzmaikin A., Sokolov D., Shukurov A., 1989, MNRAS, 241, 1

Schlickeiser R., 1989, ApJ, 336, 243

Schlickeiser R., 2002, Cosmic Ray Astrophysics. Springer, Berlin

Schlickeiser R., Miller J. A., 1998, ApJ, 492, 352

Spitzer L., 1962, Physics of Fully Ionized Gases. Interscience Publications, New York

Stawarz, Ł., Petrosian V., 2008, ApJ, 681, 1725

Tsytovich V. N., 1972, An Introduction to the Theory of Plasma Turbulence. Pergamon Press, Oxford

Tverskoi B. A., 1977, Soviet Phys. JETP, 25, 317

Yan H., Lazarian A., 2004, ApJ, 614, 757

Zatsepin G. T., Kuzmin. A., 1966, JETP Lett., 4, 78

This paper has been typeset from a TEX/LATEX file prepared by the author.